NASA Technical Memorandum 105336

Analysis of Aircraft Engine Blade Subject to Ice Impact

E.S. Reddy and G.H. Abumeri
Sverdrup Technology, Inc.
Lewis Research Center Group
Brook Park, Ohio

and

C.C. Chamis and P.L.N. Murthy
National Aeronautics and Space Administration
Lewis Research Center
Cleveland, Ohio

Prepared for the
Ninth Conference on Fibrous Composites in Structural Design
cosponsored by DoD, NASA, and FAA
Lake Tahoe, Nevada, November 4–7, 1991

NASA

ANALYSIS OF AIRCRAFT ENGINE BLADE SUBJECT TO ICE IMPACT

E.S. Reddy and G.H. Abumeri
Sverdrup Technology, Inc.
Lewis Research Center Group
Brook Park, Ohio 44142

and

C.C. Chamis and P.L.N. Murthy
National Aeronautics and Space Administration
Lewis Research Center
Cleveland, Ohio 44135

ABSTRACT

The ice impact problem on the engine blade made of layered composite is simulated. The ice piece is modeled as an equivalent spherical object and has the velocity opposite to that of the aircraft with direction parallel to the engine axis. Near the impact region and along the leading edge, the blade is assumed to be fully stressed and undergoes large deflection. A specified portion of the blade around the impact region is modeled. The effect of ice size and velocity on the average leading edge strain are investigated for a modified SR-2 model unswept composite propfan blade. Parametric studies are performed to study the response due to ice impact at various locations along the span. Also, the effects of engine speed on the strain and impact displacements are discussed. It is found that for a given engine speed, a critical ice speed exists that corresponds to the maximum strain and this critical speed increases with increase in the engine speed.

LIST OF SYMBOLS

A, B	coefficients in the displacement recursive relation
A',B'	coefficients in the velocity recursive relation
a, b	lower and upper radii for the impact modeling region
d	chordwise nodal distance from the leading edge
E_{11}, E_{22}	Modulus of Elasticity in *11* and *22* directions *(psi)*
F, G	displacement responses to unit initial displacement and unit initial velocity
F', G'	velocity responses to unit initial displacement and unit initial velocity
f	impact force
f_i	impact force on i^{th} nodal
f_{av}	impact force normal to blade chord *(lb)*
G_{12}	Modulus of Rigidity in *12* direction *(psi)*
h	time step *(sec)*
[K]	element stiffness
K_i	i^{th} component of generalized stiffness
M_i	i^{th} component of generalized mass
n	number of materials
P_i	i^{th} component of generalized force
r	equivalent radius of ice piece
T	impact load duration *(sec)*
t, τ	time *(sec)*
t_e	element thickness *(inches)*
t_n	time at n^{th} time step *(sec)*
V_{rel}	impact relative velocity *(inches/sec)*
x_i, y_i	element nodal coordinates (Figure 4 and Eq. 1) or nodal coordinates with respect to impact node (Figure 6a)

ν_{12} Poisson's ratio in *12* direction

θ impact angle relative to the blade chord

ρ density $(lb.sec^2/in^4)$

σ_{yield} element yield stress

ω_i natural frequency *(radians)*

ξ_i i^{th} modal coordinate

$\dot{\xi}_i$ velocity of i^{th} modal coordinate

$\ddot{\xi}_i$ acceleration of i^{th} modal coordinate

$\xi_{i,n}$ i^{th} modal coordinate value at n^{th} time step

$\dot{\xi}_{i,n}$ velocity value of i^{th} modal coordinate at n^{th} time step

INTRODUCTION

At high altitudes, when aircraft flies through clouds of super-cooled water droplets, ice formation occurs on forward facing structural components. One such component is the engine inlet. With time, the ice accretes on the inlet and eventually sheds due to structural vibrations. A schematic of this phenomenon is shown in Figure 1. As a result, blocks of ice travelling at the speed of aircraft impacts the engine blades rotating at high RPM. This process may cause severe damage to the blade and subsequently to the engine. In order for the blade to sustain the ice impact, it is necessary to properly account for these constraints during the design.

Fibrous composites are ideal for structural applications such as high performance aircraft engine blades where high strength-to-weight and stiffness-to-weight ratios are required. These factors along with the flexibility to select the composite layup and to favorably orient fiber directions help limit the impact damage and stresses arising from large rotational speeds.

The objective of this paper is to simulate ice impact on an engine blade. SR-2 unswept composite propfan blade is considered for local damage analysis. The impact analysis is carried out by modifying the foreign object damage option provided in Reference [1]. It is assumed that the damage is severe in the local region and hence only a specified portion of the blade around the impact region is modeled. Furthermore, large scale deflections accompany the impact event in the impact zone [2]. In order to simulate this behavior near the impact region and along the leading edge, the blade is assumed to be fully stressed and undergoes large deflection. This is accomplished in the code by modifying the membrane stiffness in the radial direction to reflect a fully yielded condition. A detailed justification for these assumptions is also given in Reference [2]. Parametric

studies are performed to study the response of the blade due to ice impact at various locations along the span. The effect of ice size and velocity on the average leading strain and maximum impact displacements are investigated.

IMPACT ANALYSIS

Geometry of Ice Impact

The geometry of ice impact on the leading edge of the blade is shown in Figures 2(a,b). Impact velocity direction relative to the blade is a function of aircraft speed and the rotational speed of the blade (Figure 2a). The resulting impact force not only depends on the magnitude and direction of relative velocity but also on the mass of ice piece. Depending on the spacing (i.e., number) of blades and relative velocity as shown in Figure 2b, only a portion of the ice piece hits the blade . The ice piece that is approaching the blade under consideration is sheared off by the adjacent blade and only a part of it impacts the leading edge. Effectively, the size of the ice piece that finally impacts the blade depends on the blade spacing, blade speed and aircraft speed.

Modeling of the Blade

The damage due to impact is considered to be highly localized and hence only a local patch: portion of the blade around the impact region (i. e., a specified portion along the span and half of the blade along the chord as shown in Figure 3) is modeled. In the code, the blade geometry is input in the form of finite element grid and nodal thicknesses. The spanwise impact region is specified with two parameters, namely, lower and upper bounds of radial fractions, a and b. However, the modeled impact span is approximated to be the region between the two finite element radial stations that are defined in the

blade geometry and are nearest to a and b. Along the chord, only half of the blade is considered for impact analysis. The finite element used is similar to NASTRAN (TRIA3) three node triangular plate element [3,4]. A total of 35 nodes and 48 elements are used (Figure 3). The impact is considered at the midpoint of the local patch (finite element node 16) along the leading edge. All the edges except the leading edge are considered fixed as the impact response beyond these boundaries is negligible.

Large scale deflections usually accompany the impact event. This phenomenon is simulated in the elements that are close to the impact node by modifying the membrane stiffness in the radial direction (to reflect fully yielded condition) and zeroing-out the spanwise bending stiffness. These special elements are shown as shaded in the Figure 3. If σ_{yield} is the effective yield stress of the element in the radial direction, w_1, w_2 and w_3 are out of plane displacements at 3 nodes, the modified stiffness associated with these degrees of freedom is given by [2],

$$[K] = \frac{y_3}{2x_2}\sigma_{yield}\, t_e \begin{bmatrix} 1 & -1 & 0 \\ -1 & 1 & 0 \\ 0 & 0 & 0 \end{bmatrix} \qquad (1)$$

where t_e is the element thickness and x_2 and y_3 are the element local coordinates (Figure 4). The terms of this stiffness matrix replace the spanwise bending stiffnesses of linear elastic triangle. The stiffness in Equation (1) reflects the perfectly plastic condition with constant stress (σ_{yield}) in the radial direction.

Figure 5 shows the material configuration of the composite blade. In each finite element, the skin (material *1*) is always present. The remaining materials exist only if the blade thickness permits them. Materials *(n-1), (n-2)* ,.. are dropped from the layup of an element in that order. If the element thickness can accommodate all the materials then

the core (n^{th} material with variable thickness) is used to fill the remaining excess thickness.

Modeling of Ice Impact Loading

The impact force on the blade arises from the momentum of the ice piece. The temporal and spatial distribution of this impact force is carried out with the following considerations [2]:

a) Only the impact force component normal to the blade chord will cause the local deformation.

b) Load duration, T, of impact is the time taken by the equivalent spherical ice piece (radius, r and relative velocity, V_{rel}) to squash-up, i. e., $T = 2\,r / V_{rel}$.

c) Impact force is distributed using a parabolic distribution function over all finite element nodes within one diameter (equivalent) of the ice piece from the impact node (see Figures 6a and 6b).

$$f_i = \frac{f_{av}\,[1 - x_i^2/4r^2]\,[1 - y_i/2r]}{\sum_{i \in \Pi} [1 - x_i^2/4r^2]\,[1 - y_i/2r]} \qquad (2)$$

where f_i is the nodal force, f_{av} is the component of the impact force normal to the blade chord, x_i and y_i are the local coordinates with impact node as the origin (Figure 6a).

d) The impact wave travels along the chord at the same velocity as that of ice impact. As a result, i^{th} nodal loading start time, T_i , is defined by the ratio of nodal chordwise distance, d from the leading edge and the ice relative velocity, V_{rel}, i.e., $T_i = d/V_{rel}$, (see Figure 6a).

e) Blade flexibility reduces the instantaneous ice impact loads due to reduction in the relative velocity. However, deflection of the blade results in ingestion of extra ice and therefore, there is an increase in the total momentum exchange. These factors are accounted and nodal forces are adjusted accordingly (see Reference [2] for details).

Transient Response Analysis

Transient response of the local patch is obtained by the process of modal integration. The modal analysis is based on the principle that statically deformed structure can be described by a combination of that structure's mode shapes. Once the coefficient of each mode's participation is calculated, the impact event can be simulated by the integration of a series of linear steps through time. The deflected shape due to ice impact is basic; therefore, only the first five modes of the local patch are used to compute the response. Also, damping is assumed to be zero as very little structural damping occurs during the impact event.

Upon diagonalizing the governing equations of motion of undamped system [5], the uncoupled equations with each modal coordinate, ξ_i, satisfies the second order differential equation,

$$\ddot{\xi}_i + \omega_i^2 \xi_i = \frac{1}{M_i} P_i(t) \qquad (3)$$

where $\omega_i^2 = K_i/M_i$, M_i and K_i are the i^{th} diagonal elements of the generalized mass and stiffness matrices, and $P_i(t)$ is the i^{th} component of the generalized force at time t.

The general solution of the above equation, expressed in terms of arbitrary initial conditions, $\xi_{i,n}$ and $\dot{\xi}_{i,n}$ at $t = t_n$, and a convolution integral of the applied load, is,

$$\xi_i(t) = F(t-t_n)\xi_{i,n} + G(t-t_n)\dot{\xi}_{i,n} + \frac{1}{M_i}\int_{t_n}^{t} G(t-\tau)\, P_i(\tau)\, d\tau \qquad (4)$$

where F and G, respectively, the solutions with unit displacement and unit velocity initial conditions.

Assuming that load varies linearly between t_n and t_{n+1}, solution at time t_{n+1} can be obtained in closed form as (see Reference [6]),

$$\xi_{i,n+1} = F(h)\xi_{i,n} + G(h)\dot{\xi}_{i,n} + A\, P_{i,n} + B\, P_{i,n+1} \qquad (5a)$$

$$\dot{\xi}_{i,n+1} = F'(h)\xi_{i,n} + G'(h)\dot{\xi}_{i,n} + A'\, P_{i,n} + B'\, P_{i,n+1} \qquad (5b)$$

where $h = t_{n+1} - t_n$, $F(h) = \cos\omega_i h$, $G(h) = (1/\omega_i)\sin\omega_i h$, $F'(h) = -\omega_i \sin\omega_i h$ and $G'(h) = \cos\omega_i h$ for undamped system [5].

For zero initial conditions ($\xi_{i,0} = \dot{\xi}_{i,0} = 0$), the coefficients A, A', B and B' are given by

$$A = \frac{1}{M_i\omega_i^2}\left\{\frac{\sin\ \omega_i h}{\omega_i h} - \cos\ \omega_i h\right\},\ B = \frac{1}{M_i\omega_i^2}\left\{1 - \frac{\sin\ \omega_i h}{\omega_i h}\right\} \qquad (6a)$$

$$A' = \frac{1}{M_i\omega_i}\left\{sin\ \omega_i h - \frac{1}{\omega_i h} + \frac{cos\ \omega_i h}{\omega_i h}\right\},\ B' = \frac{1}{M_i\omega_i}\left\{\frac{1}{\omega_i h} - \frac{cos\ \omega_i h}{\omega_i h}\right\} \qquad (6b)$$

The response at all time steps can be obtained by applying equations for $\xi_{i,n+1}$ and $\dot{\xi}_{i,n+1}$ recursively. At each time step, the modal coordinates, $\xi_{i,n}$, can be transformed to nodal displacements using modal matrix. From these displacements, large radial strains, ε_x, of the leading edge elements are computed with the relation [2],

$$\varepsilon_x = \frac{1}{2}\left[\frac{w_2 - w_1}{x_2}\right]^2 \qquad (7)$$

The entire calculation proceeds very quickly, due to the uncoupled nature of the modal responses. Among the strains at all the time steps, the maximum is picked as a representative quantity for the local impact damage.

RESULTS AND DISCUSSION

The SR-2 model unswept propfan blade [7] is chosen to study the ice impact and the planform of the blade is shown in Figure 7. The setting angle (orientation of the blade chord with respect to the plane of rotation at 75% span) is 57° and the number of blades are 8. In the present study, the composite material layup: Titanium skin/Graphite-Epoxy (±45)/Titanium core is used (Figure 8). For these materials, the properties are given in Table 1. The effective yield stress for element stiffness modification is assumed to be 206 ksi.

Effect of Ice Size and Ice Velocity

The impact in the region 50-90% of the span is known to cause severe damage to the blade [2]. Hence, lower and upper limits of the modeling region are taken as 50% and 90% blade span for the impact analysis. For this modeling region, the impact radius is at 9.55" (73.5% span). These data are presented for three engine speeds, 3000, 5000 and 8000 RPM in the form of contour plots (Figures 9a-c). For all the engine speeds, the maximum strain corresponds to r = 0.8". However, the corresponding critical ice speed varies depending on the engine RPM. As an example, at 3000, 5000 and 8000 RPM the peaks are respectively at 100, 130 and 190 knots. The associated peak values of the strains are 1.66%, 7.61% and 14.22%. From these plots, a safe range of ice impact parameter, namely, ice speed and ice size that can cause a specified local damage to the blade can be determined. Once the designer determines the tolerable strain along the leading edge of the blade, the combination of ice size and speed are defined by the region to the left of the level curve labelled with that strain.

For the maximum ice size, a typical variation of strain with ice speed is shown in Figure 10. The strain is zero at ice speeds 0 and 211 knots. But it reaches a maximum value at 100 knots. This is due to the fact that only impact force normal to the chord ($f \sin\theta$) gives rise to this strain. When ice speed= 0, the impact force (f) is zero and when ice speed = 211 knots, the impact angle (θ) is zero. Initially the value of θ is equal to the stagger angle (55° at the impact radius) and gradually decreases to 0° as the ice speed increases (Figure 10).

Figure 11 shows the the effect of impact radius on the strain. The strain is nearly zero when the impact takes place below 53% span (approx. 7.5" radius) but steeply increases as the ice impacts towards the blade tip. This is expected as the blade is relatively thin closer

to the tip. Also, the blade velocity, consequently, impact force increases as the impact radius increases.

Effect of Engine Speed

With engine RPM as the parameter (1000-10,000 RPM), strain plot shown in Figure 10 is repeated in Figure 12. It can be seen that the variation of strain is smooth for engine speeds up to 4000 and fluctuates for the higher speeds. However, the average trend remains the same for all RPM and the peak strain is larger for higher engine speed. The probable cause of these local fluctuations is due to discrete nature of the nodal force distribution, i.e., the finite element nodes which are in the force distribution boundary are suddenly loaded when the impact wave reaches it (Figure 6a).

Relative magnitudes of typical impact (out-of-plane) displacement distributions for three engine speeds (3000, 5000 and 8000 RPM) are shown in Figure 13. The data corresponds to Ice speed of 200 knots and ice radius of 0.8". The displacements along the leading edge remain same and gradually decreases to zero toward the center of the blade. The maximum displacement for 5000 RPM is higher than that for 8000 RPM as the analysis ice speed (200) does not correspond to the critical one in both the cases.

CONCLUSIONS

The ice impact on an aircraft engine blade made of layered composite is simulated. From the results presented in this paper, the following conclusions can be drawn:

1. The largest ice piece results in maximum average leading edge strain.

2. For a given engine speed, a critical ice speed exists that corresponds to the maximum strain. This critical speed increases with increase in the engine speed.
3. The leading edge strain increases steeply with increase in impact radius.
4. The strains generated from this analysis can be effectively used for structural tailoring of engine blades.

REFERENCES

1. Brown, K. H.: Structural Tailoring of Engine Blades (STAEBL), User's Manual. United Technologies, Pratt & Whitney Report No. PWA-5774-39, March 1985.

2. Brown, K. H.: Structural Tailoring of Engine Blades (STAEBL), Theoretical Manual. NASA CR 175112.

3. MacNeal, R. H.: A Simple Quadrilateral Shell Element. Computers and Structures, vol. 8, Pergamon Press, Great Britain, 1978, pp. 175-183.

4. MSC/NASTRAN, Version 65C, User's Manual. The MacNeal-Schwendler Corporation, 1987.

5. Thomson, W. T: Theory of Vibration with Applications. Prentice Hall, Inc., Englewood Cliffs, New Jersey, 1981.

6. MacNeal, R. H.: The NASTRAN Theoretical Manual. NASA SP- 221 (01), 1972.

7. Reddy, T. S. R.; and Kaza, K. R. V.: Analysis of an Unswept Propfan Blade With a Semiempirical Dynamic Stall Model. NASA TM 4083, 1989.

Table 1: Properties of the Blade Constituent Materials

Material Type	E_{11} (psi)	E_{22} (psi)	G_{12} (psi)	ν_{12}	ρ ($lb.sec^2/in^4$)	ply thickness (inches)
Titanium (Ti6)	16.5×10^6	16.5×10^6	6.4×10^6	0.30	0.00044	----
Graphite-Epoxy	32.0×10^6	1.0×10^6	0.7×10^6	0.25	0.00015	0.005

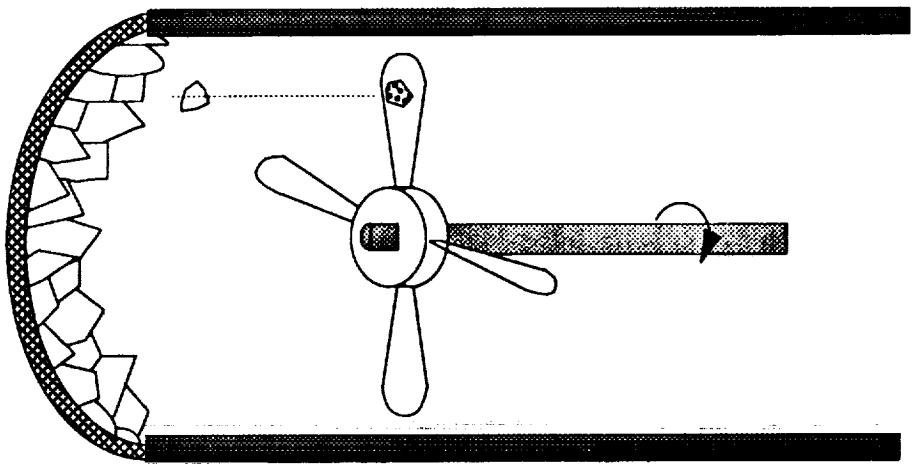

Figure 1. A Schematic of Ice Impact on an Engine Blade

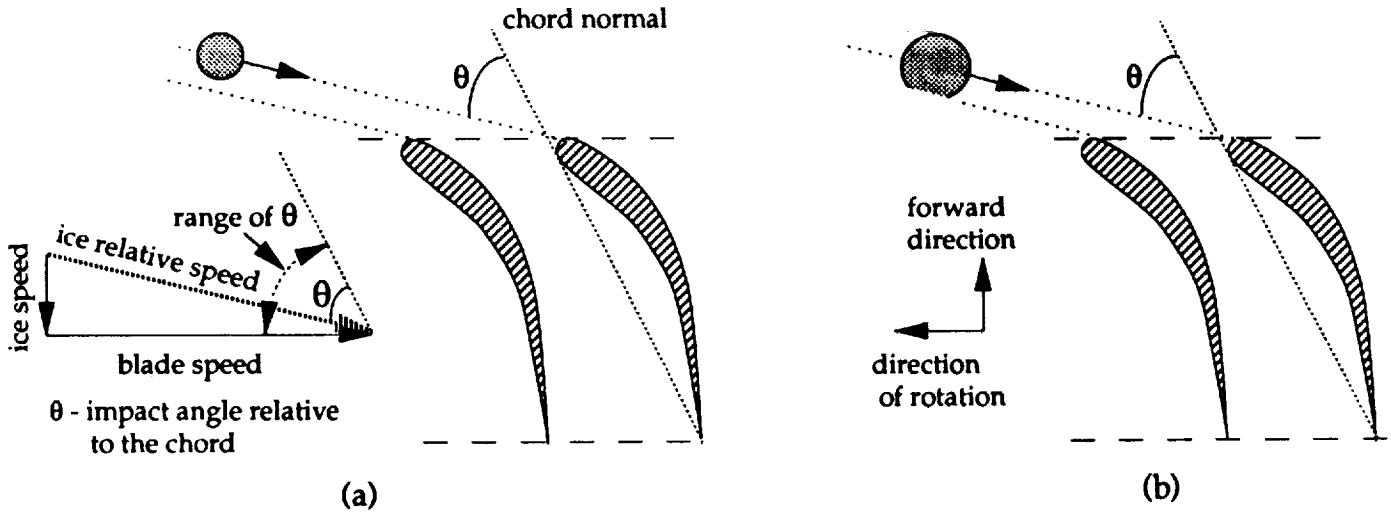

Figure 2. Geometry of Ice Impact on an Engine Blade

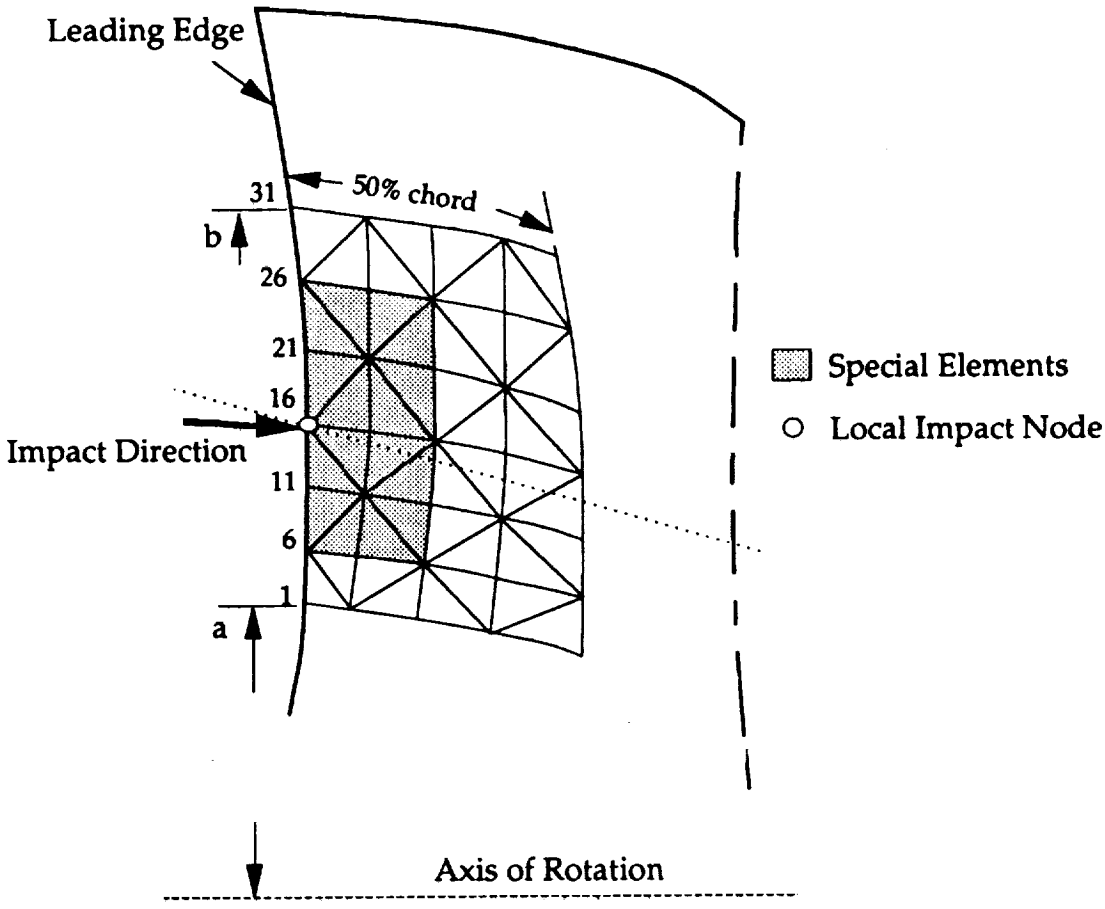

Figure 3. Finite Element Model for Local Impact Analysis

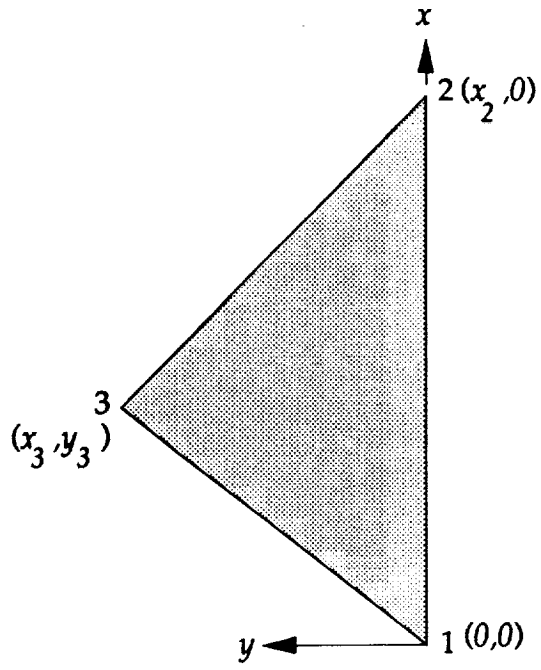

Figure 4. Finite Element Local Coordinate System

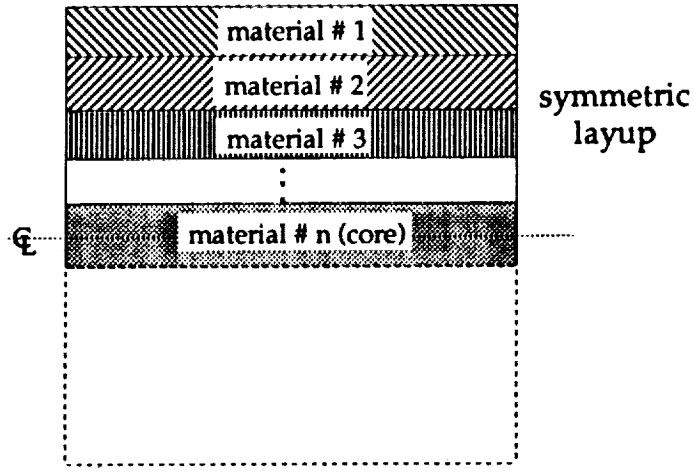

Figure 5. Symmetric Material Layer Configuration in the Composite Blade

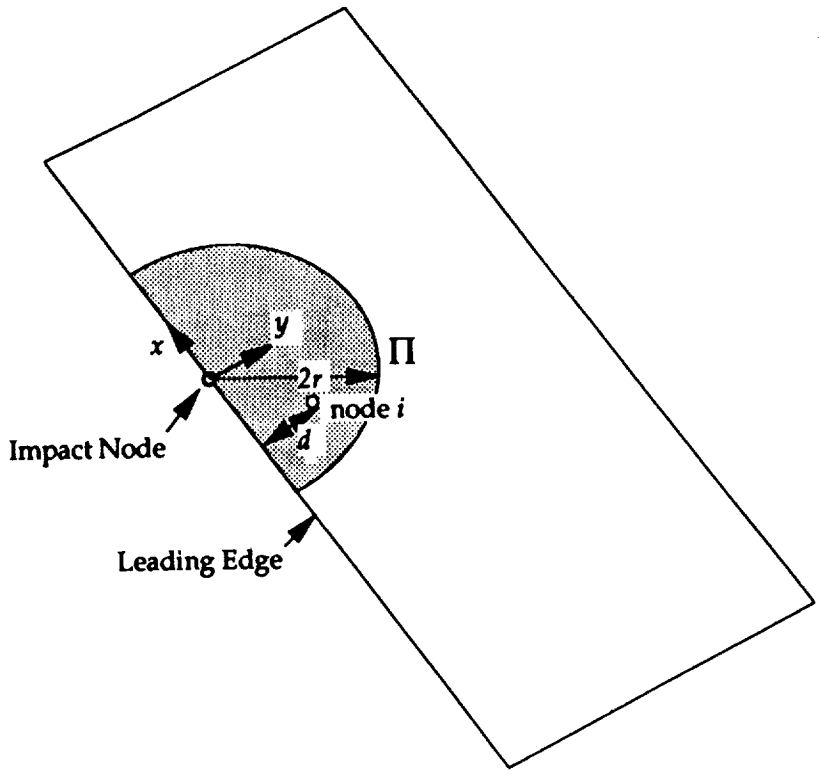

Figure 6a. Force Distribution Region in Local Impact

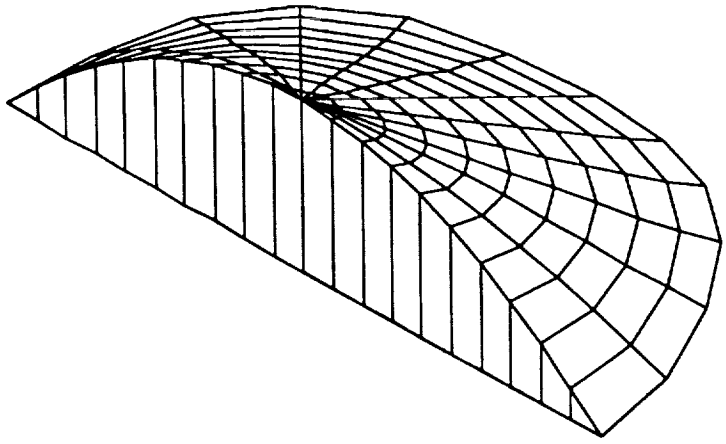

Figure 6b. Parabolic Force Distribution in the Region Π

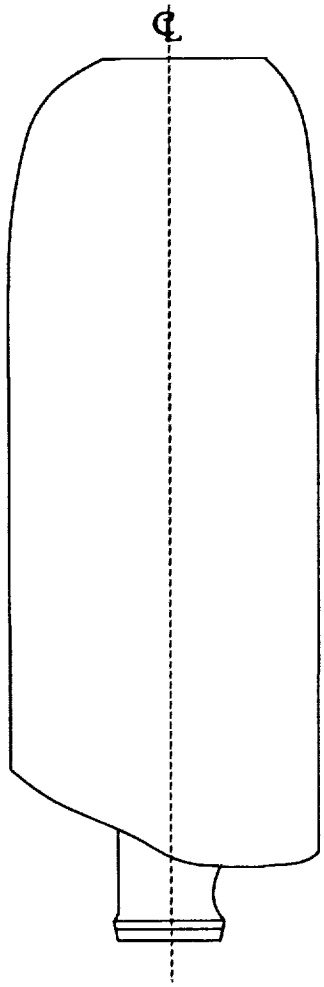

Figure 7. A Schematic of the Planform of SR-2 Model Propfan Blade

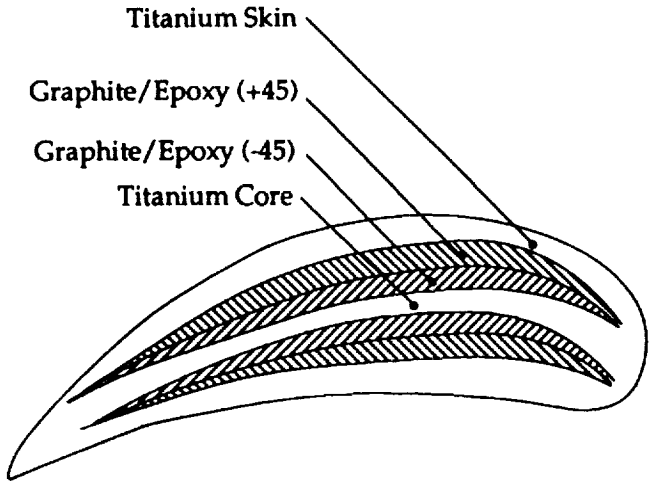

Figure 8. Material Layup of the Unswept Blade Example

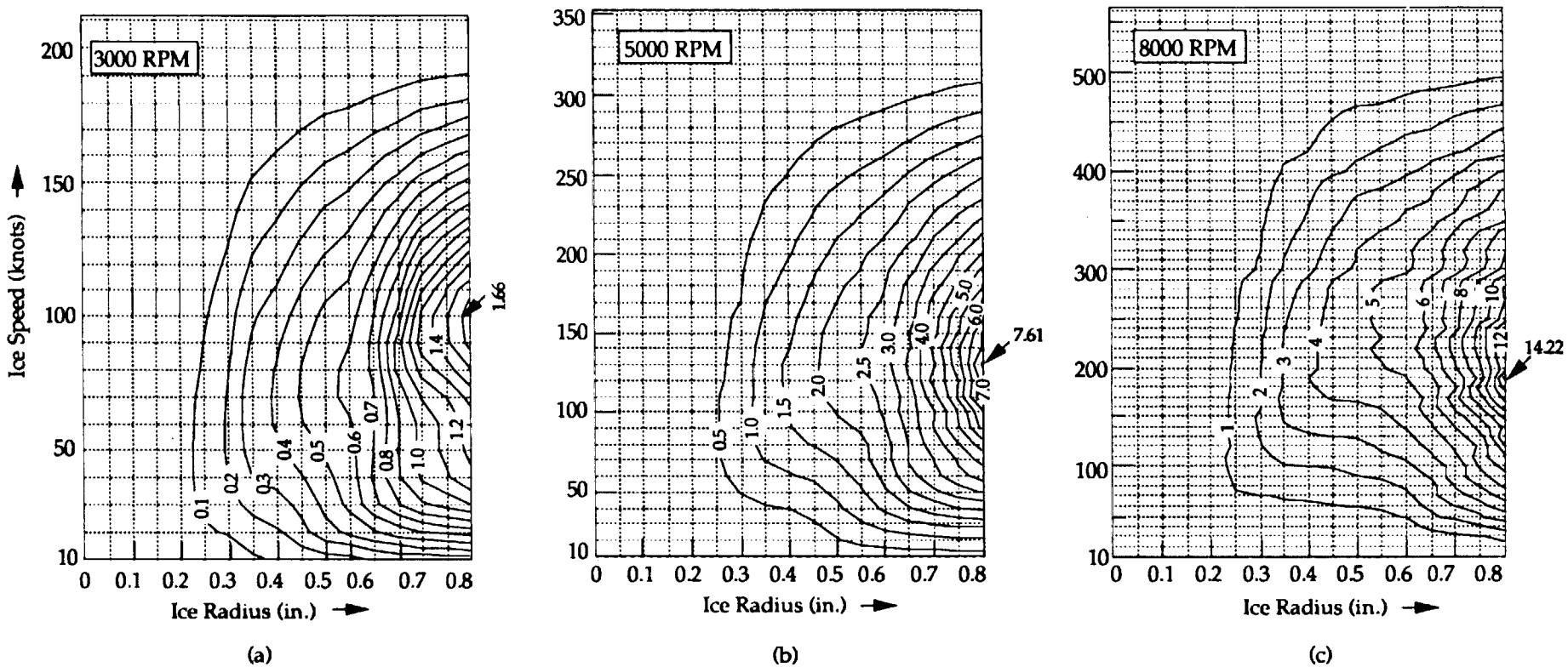

Figure 9. Average Leading Edge Strain Contours as a Function of Ice Speed and Ice Size

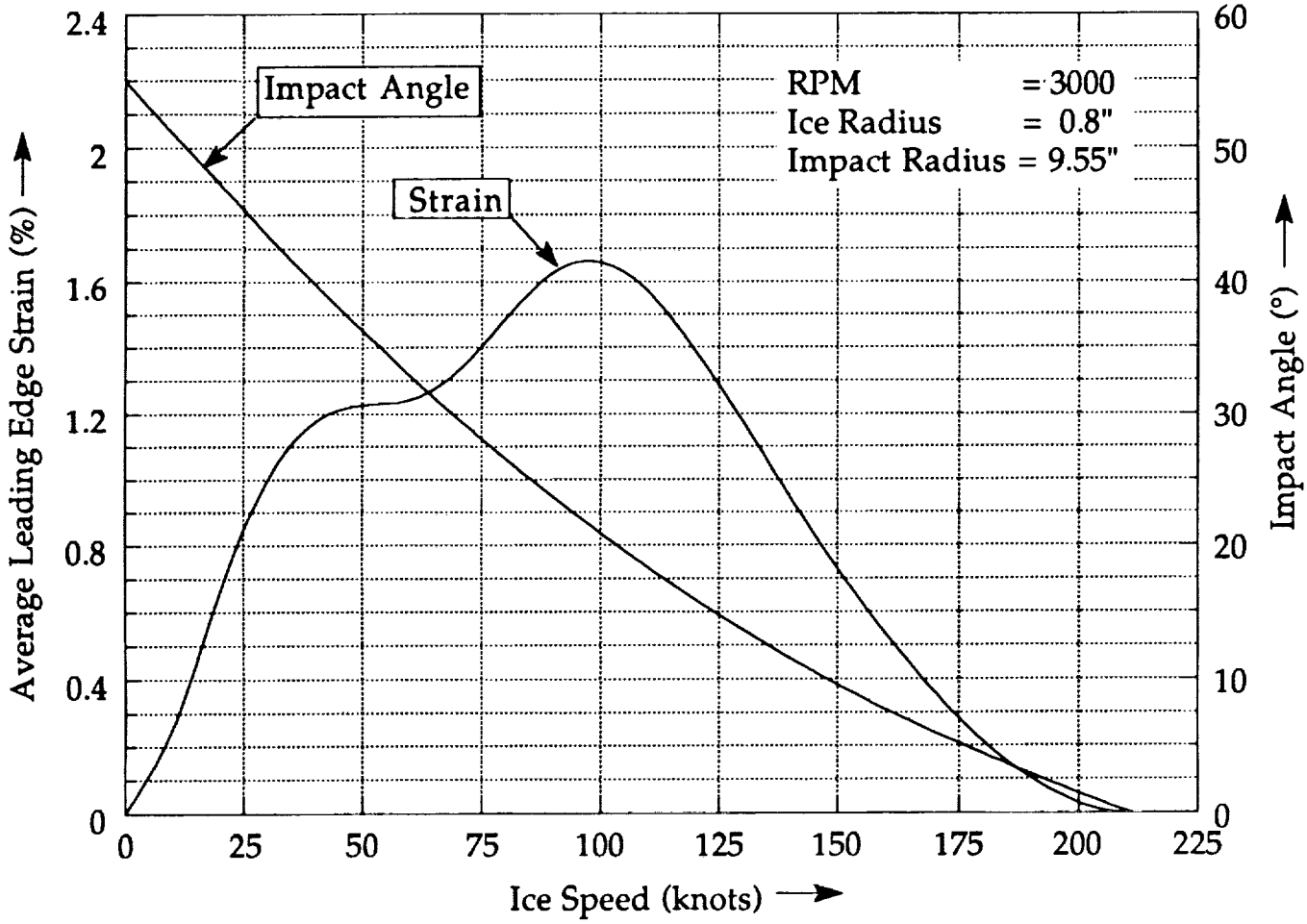

Figure 10. Variation of Average Leading Edge Strain and Impact Angle with Ice Speed

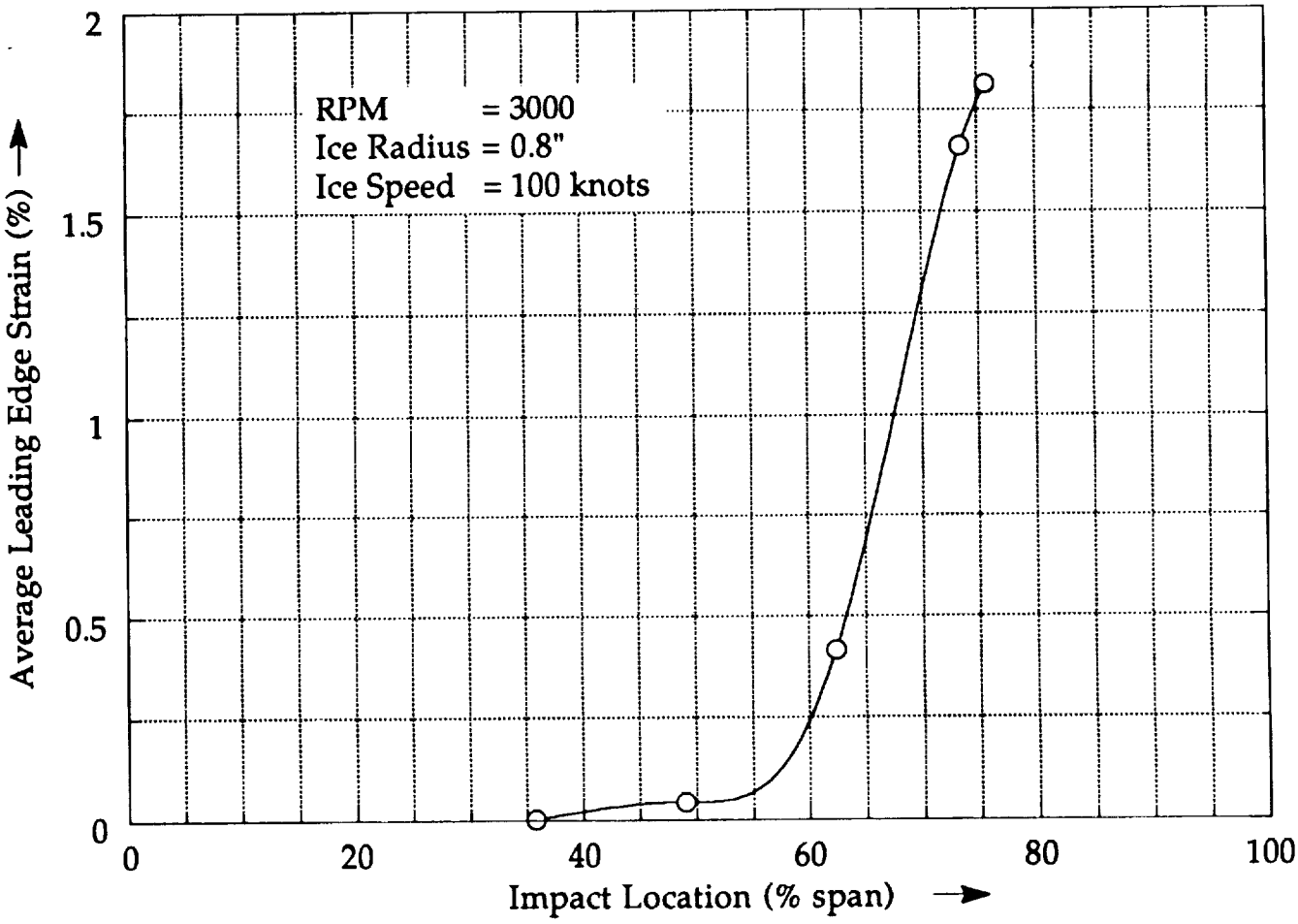

Figure 11. Effect of Impact Location on Average Leading Edge Strain

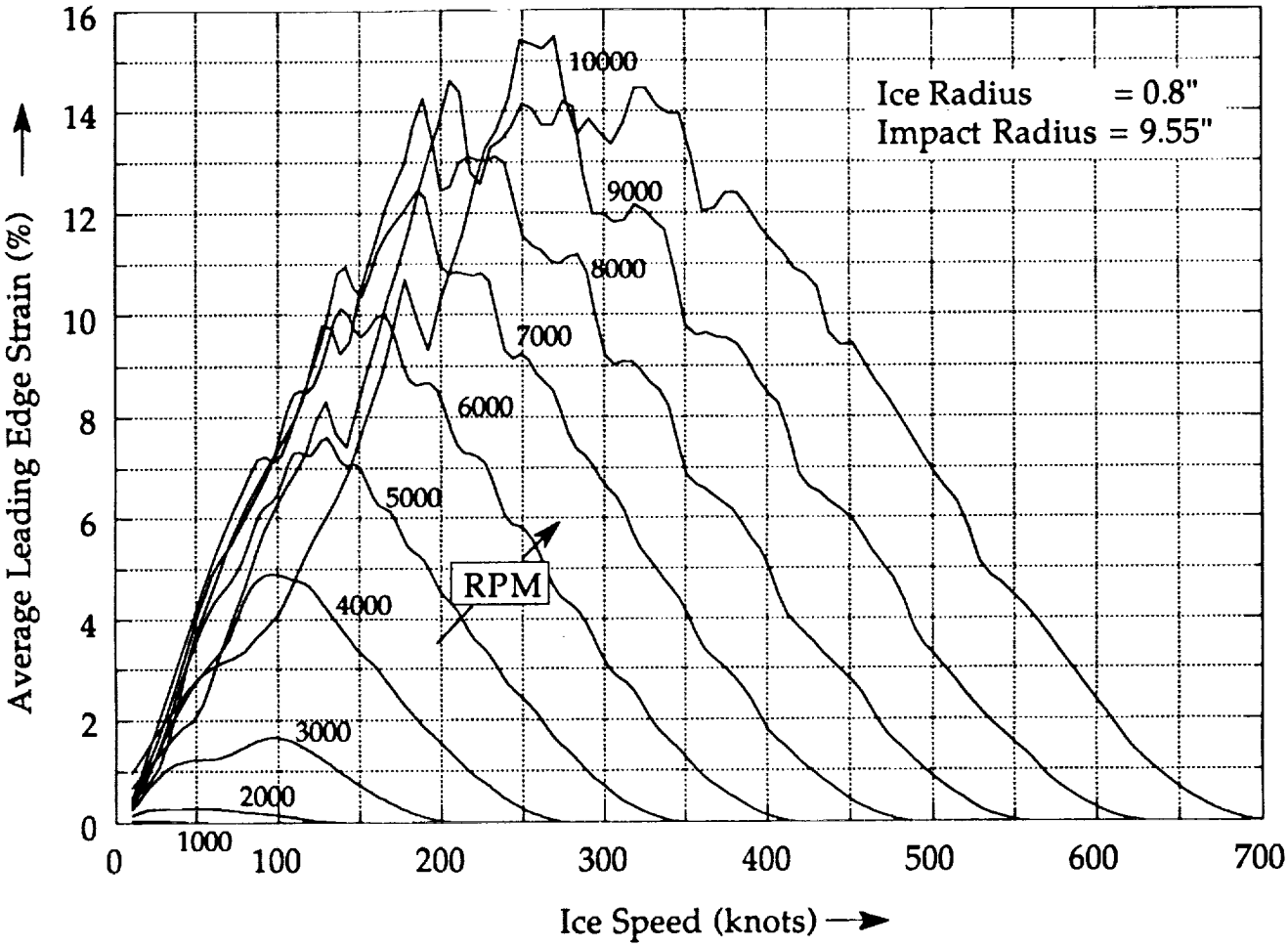

Figure 12. Effect of Ice Speed on Average Leading Edge Strain with RPM as Parameter

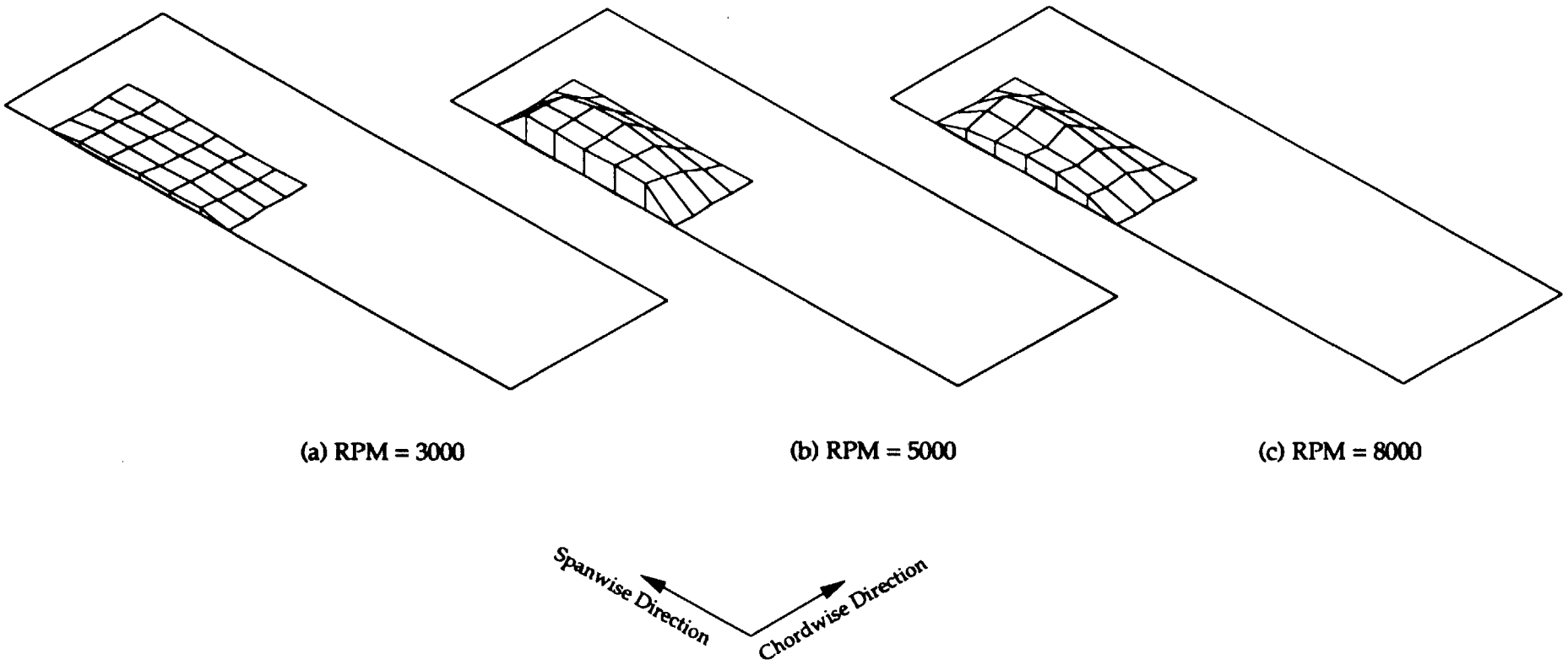

Figure 13. Absolute Out-of-Plane Displacements of Impact Region, Ice Size = 0.8",Ice Speed = 200 knots, Impact Location: 73.5% Span

REPORT DOCUMENTATION PAGE

Form Approved
OMB No. 0704-0188

1. AGENCY USE ONLY (*Leave blank*)	2. REPORT DATE	3. REPORT TYPE AND DATES COVERED
	1991	Technical Memorandum

4. TITLE AND SUBTITLE
Analysis of Aircraft Engine Blade Subject to Ice Impact

5. FUNDING NUMBERS
WU-505-68-1C

6. AUTHOR(S)
E.S. Reddy, G.H. Abumeri, C.C. Chamis, and P.L.N. Murthy

7. PERFORMING ORGANIZATION NAME(S) AND ADDRESS(ES)
National Aeronautics and Space Administration
Lewis Research Center
Cleveland, Ohio 44135-3191

8. PERFORMING ORGANIZATION REPORT NUMBER
E-6703

9. SPONSORING/MONITORING AGENCY NAMES(S) AND ADDRESS(ES)
National Aeronautics and Space Administration
Washington, D.C. 20546-0001

10. SPONSORING/MONITORING AGENCY REPORT NUMBER
NASA TM-105336

11. SUPPLEMENTARY NOTES
Prepared for the Ninth Conference on Fibrous Composites in Structural Design cosponsored by DoD, NASA, and FAA, Lake Tahoe, Nevada, November 4-7, 1991. E.S. Reddy and G.H. Abumeri, Sverdrup Technology, Inc., Lewis Research Center Group, 2001 Aerospace Parkway, Brook Park, Ohio 44142; C.C. Chamis and P.L.N. Murthy, NASA Lewis Research Center. Responsible person, C.C. Chamis, (216) 433-3252.

12a. DISTRIBUTION/AVAILABILITY STATEMENT
Unclassified - Unlimited
Subject Category 39

12b. DISTRIBUTION CODE

13. ABSTRACT (*Maximum 200 words*)
The ice impact on the engine blade made of layered composite is simulated. The ice piece is modeled as an equivalent spherical object and has the velocity opposite to that of the aircraft with direction parallel to the engine axis. Near the impact region and along the leading edge, the blade is assumed to be fully stressed and undergoes large deflection. A specified portion of the blade around the impact region is modeled. The effect of ice size and velocity on the average leading edge strain are investigated for a modified SR-2 model unswept composite propfan blade. Parametric studies are performed to study the response due to ice impact at various locations along the span. Also, the effects of engine speed on the strain and impact displacements are discussed. It is found that for a given engine speed, a critical ice speed exists that corresponds to the maximum strain and this critical speed increases with increase in the engine speed.

14. SUBJECT TERMS
Fan blades; Fiber composites; Impact damage; Impact loads; Transient response; Finite element method

15. NUMBER OF PAGES
24

16. PRICE CODE
A03

17. SECURITY CLASSIFICATION OF REPORT	18. SECURITY CLASSIFICATION OF THIS PAGE	19. SECURITY CLASSIFICATION OF ABSTRACT	20. LIMITATION OF ABSTRACT
Unclassified	Unclassified	Unclassified	